



## UTILIZING ARTIFICIAL NEURAL NETWORKS TO ANTICIPATE EARLY-AGE THERMAL PARAMETERS IN CONCRETE PIERS

Hoàng Việt Hải<sup>1</sup> \*, Đỗ Anh Tú<sup>1</sup>, Phạm Đức Thọ<sup>2</sup>

<sup>1</sup>Faculty of Civil Engineering, University of Transport and Communications, 3 Cau Giay, Lang Thuong, Dong Da, Hanoi, Vietnam

<sup>2</sup>Faculty of Civil Engineering, Hanoi University of Mining and Geology, No.18 Vien Street, Duc Thang Ward, Bac Tu Liem District, Ha Noi, Vietnam

### ARTICLE INFO

TYPE: Research Article

Received: 13/12/2022

Revised: 15/02/2023

Accepted: 14/05/2023

Published online: 15/05/2023

<https://doi.org/10.47869/tcsj.74.4.5>

\* *Corresponding author*

Email: hoangviethai@utc.edu.vn; Tel: +84902385538

**Abstract.** Recently, researches have been used Artificial Neural Network (ANN) to predict the early-age thermal cracking of rectangle piers. But ANN has not resulted for different types of concrete piers. This article presents an evaluation of the early-age thermal characteristics of mass concrete piers with four distinct cross-sectional shapes. A finite element (FE) model was employed to estimate the maximum temperature, thermal stress, and cracking potential of the concrete pier at its early age. To investigate the impact of various pier geometries on the thermal cracking potential, different pier geometries were considered. In this study, an ANN model was utilized to predict the maximum temperature and decrease the risk of cracking in mass concrete piers at early age. The database of thermal mass concrete piers used in this study comprises 128 results obtained from the FE model. The results of the analysis indicate that the ANN model can predict early-age thermal parameters, and cracking risk in early-age concrete piers with good accuracy and help to the designer to choose the appropriate size in minimizing cracks on the pier concrete.

**Keywords:** Mass concrete pier, maximum temperature, temperature difference, artificial neural network (ANN), thermal crack.

## 1. INTRODUCTION

Large concrete structures such as bridge foundations, piers, and abutments are often classified as “mass concrete” [1, 2]. When a larger volume of fresh concrete is cast in place, a larger amount of heat releases from the cement hydration process. The temperature at the inside portion of the concrete is increasing while that at the surface is quickly decreasing due to the high convection with the air. This phenomenon creates a large temperature difference between the core and the outer surface of the concrete, leading to high thermal tensile stresses that may exceed the concrete tensile strength that develops versus time, which will cause thermal cracks [3-5]. When cracking occurs in the concrete, it accelerates the corrosion of reinforcement in structure concrete and affect the durability of the structure. Therefore, it is necessary to analyze the temperature and the thermal stress in mass concrete structures for controlling temperature and preventing crack initiation in the early-age concrete [6].

In order to reduce a large difference temperature and tensile stress due to heat in masse concrete, it is common to reduce the amount of cement in the mixture, reduce the temperature of the aggregates and the water before mixing [7, 8], and casting concrete at night or in the early morning [6]. In addition, for abutments and bridge footing, when its geometry is large, the designers are arranged with a cool piping system to reduce the heat in the concrete [9]. However, for the piers, all designs do not have this system arrangement in order to minimize cracking in mass concrete. One of the solutions considered is the structural solution, by changing the shape of the pier body to minimize cracking. In this study, 3D Finite Element Modeling was firstly used to investigate the influence of geometrical factors on maximum temperature, temperature difference, and cracking risk in the structure, ... then study using artificial intelligence simulation applied in thermal analysis in large concrete structure

In recent years, Artificial Neural Network (ANN) has been applied effectively in many fields related to materials and structures [10-13], ANN is now one of the most popular models due to its structural flexibility, excellent prediction performance, and the availability of a number of training algorithms [14]. Recent research used ANN to predict the early-age thermal cracking of rectangle piers [15] but it has not resulted for different types of concrete piers. In this study, an artificial neural network (ANN) model is proposed to control temperature and reduce cracking risk in mass concrete piers. The thermal mass concrete piers database in this study includes 128 results from FE model. The performance of this models is also discussed.

## 2. FE Modeling for Heat Generation and Transfer in Concrete Pier

### 2.1. FE basis for solving heat transfer problem

The FE formulation for the problem of conduction heat transfer can be developed using the conservation of energy principle [16].

$$\frac{\partial}{\partial x} \left( \lambda_x \frac{\partial T}{\partial x} \right) + \frac{\partial}{\partial y} \left( \lambda_y \frac{\partial T}{\partial y} \right) + \frac{\partial}{\partial z} \left( \lambda_z \frac{\partial T}{\partial z} \right) + q_v = \rho c \frac{\partial T}{\partial t},$$

where  $\rho$  = density of concrete;  $\lambda$  = concrete thermal conductivity;  $c_p$  = concrete specific heat;  $T$ = concrete temperature;  $t$  = time;  $\dot{Q}$  = heat rate; and  $x$ ,  $y$ , and  $z$  = coordinates

Two types of heat transfer boundary conditions are often used to analyze heat problems, which are expressed by Equations (1) and (2) [16]:

$$T = T_p, \quad (1)$$

$$\lambda_x \frac{\partial T}{\partial x} L_x + \lambda_y \frac{\partial T}{\partial y} L_y + \lambda_z \frac{\partial T}{\partial z} L_z + q_v + h(T_s - T_f) = 0, \quad (2)$$

where  $T_p$  is the temperature of the surface or concrete pier ( $^{\circ}\text{C}$ ),  $q_v$  is the heat generated per unit volume ( $\text{kcal}/\text{m}^3$ ),  $h$  is the convective coefficient ( $\text{kcal}/\text{m}^2 \cdot \text{h} \cdot ^{\circ}\text{C}$ ),  $T_s$  is the temperature of concrete pier ( $^{\circ}\text{C}$ ),  $T_f$  is the ambient temperature ( $^{\circ}\text{C}$ ),  $L_x$ ,  $L_y$ , and  $L_z$  are the directional cosine of the surface according to the  $x$ ,  $y$  and  $z$  axes, respectively.

The problem of heat transfer is solved using the following matrix equation [16]:

$$[\lambda]\{T\} + [C]\left\{\frac{\partial T}{\partial t}\right\} = [Q], \quad (3)$$

In order to treat the problem of unstable heat transfer, it is necessary to analyze time into steps  $\Delta t$  as follows:

$$\left\{\frac{\partial T}{\partial t}\right\} = \frac{1}{\Delta t} [T(t_n) - T(t_{n-1})], \quad (4)$$

Equation (5) is obtained by combining Equations (3) and (4) and expressed as follows:

$$[\lambda]\{T\} + \frac{[C]}{\Delta t} [T(t_n) - T(t_{n-1})] = [Q], \quad (5)$$

where  $[\lambda]$  is conductivity operator,  $[C]$  is capacity operator, and  $[Q]$  is heat load due to heat of hydration,  $\Delta t = \Delta t_n - \Delta t_{n-1}$  is the time step.

Solving Equation (5) gives temperature fields in the concrete block at different time steps.

Thermal stress in the concrete is determined by Equation (6):

$$\{\sigma\} = [E][B]\{u\} = [E](\{\varepsilon\} - \{\varepsilon^{th}\}), \quad (6)$$

where  $\{\sigma\}$  is the thermal stress vector,  $[E]$  is the elasticity matrix,  $[B]$  is the strain-displacement matrix, based on the element shape functions,  $\{u\}$  is the nodal displacement vector,  $\{\varepsilon\}$  is the strain vector, and  $\{\varepsilon^{th}\}$  is the thermal strain vector.

The determination of temperature field in a mass concrete structure is a complex problem because it depends not only on the shape of the structure but also on other factors such as the internal heat generation, the ambient temperature, .... In recent years, numerical approaches such as finite difference and FE methods have been widely used to predict temperature and stress fields in mass concrete structures [4, 17]. In this study, the Midas/Civil software [18] based on the FE method was used to model the early-age behavior of the concrete pier. The research of Hồ Ngọc Khoa [19] was used this software to compared the simulation results with the experimental measurement results of mass concrete having dimensions of  $4\text{m} \times 4\text{m} \times 4,6\text{m}$ . The results are in close agreement.

## 2.2. Description of the mass concrete piers

In this study, 4 type of concrete piers casting in place is modelled (Figure 1). The concrete footing is assumed to have dimensions of  $16\text{m} \times 12\text{m} \times 3\text{m}$ . The pier concrete has two planes of symmetry, therefore only one-quarter of the pier is analyzed in order to reduce the computation

time. The geometry and dimensions of the pier are shown in table 1.

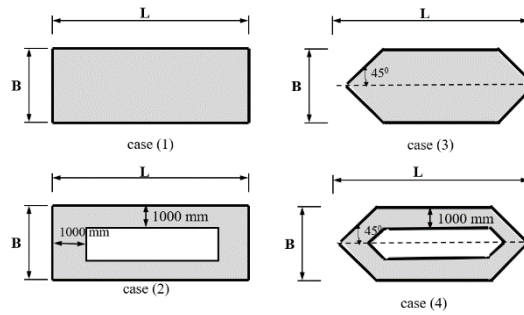


Figure 1. Pier Cross-section Shapes.

Table 1. Geometry and dimensions of the piers.

L (m)	B(m)	H(m)
3	1	6
4	2	
5	3	
6	4	
7		
8		
9		
10		
8 combinations of length		4 combinations of width
		1 combinations of height
R=B/2; b=1(m) and $\alpha=45^0$ degree		

As shown in Figure 1 and Table 1, It can be noted that 8 (combinations of length) x 4 (combinations of width) x 4 (type of piers) = 128 samples.

The temperature of the foundation of pier is considered 27°C and the initial concrete temperature of concrete pier is assumed to be 27°C. The thermal and physical characteristics of the pier concrete and the concrete pier footings used in the analysis are presented in Table 2.

Table 2. Thermal and mechanical properties of concrete and soil foundation.

Property	Concrete	Concrete pier footing
Thermal conductivity (kcal/kN*°C)	25	25
Specific heat capacity (kcal/m*h*°C)	2.3	2.3
Density (kg/m <sup>3</sup> )	2400	2400
Surface convection coefficient (kcal/m <sup>2</sup> *h*°C)		
- Boundary 1 (free contact with air)	12.00	
- Boundary 2 (steel shuttering)	12.00	12.00
- Boundary 3 (free contact in piers corps)	3	
Coefficient of thermal expansion (/°C)	10 <sup>-5</sup>	10 <sup>-5</sup>
Modulus of elasticity (kN/m <sup>2</sup> )	2.98×10 <sup>7</sup>	2.98×10 <sup>7</sup>
Poisson's ratio	0.20	0.2
Design compressive strength, (MPa)	35.00	-
Ambient temperature (°C)	27	

ACI 318-19 [20] suggests the following expressions (Eqs. (7) and (8)) for estimating splitting tensile strength and Young’s modulus as functions of the compressive strength:

$$f_{sp}(t) = 0.56\sqrt{f_c'} \tag{7}$$

$$E(t) = 4700\sqrt{f_c'} \tag{8}$$

$$f_c'(t) = \frac{t_{eq} \cdot f_c'}{a + b \cdot t_{eq}} \tag{9}$$

where  $f_{sp}(t)$  is the splitting tensile strength (MPa),  $E(t)$  is the Young’s modulus (MPa),  $f_c'(t)$  is the compressive strength (MPa) at  $t_{eq}$  days,  $f_c'$  is the compressive strength (MPa) at 28 days and  $a, b$  are constants and equal to 1.2 , 0.85, respectively.

### 2.3. Crack index for evaluation of early-age cracking risk

The prediction of crack formation in an early-age concrete structure plays an important role in minimizing the cracking risk and/or controlling crack growth. Criteria for evaluating early-age thermal cracking in concrete vary from country to country [8]. In the United States, the ACI guidelines for assessing thermal cracking are not specified except for a recommended limiting value for the temperature difference between the core and the outer surface of the concrete. In other countries such as Korea and Japan, “crack index” is preferably used as a measure for assessing early-age cracking potential in the concrete. Crack index is determined by Equation (10):

$$I_{ct} = \frac{f_{sp}(t)}{f_t(t)} \tag{10}$$

where  $I_{ct}$  is the crack index,  $f_t(t)$  is the maximum tensile stress (MPa), and  $f_{sp}(t)$  is the splitting tensile strength of the concrete (MPa).

The tendency of cracking can be evaluated using “crack index” based on engineering experience as introduced in Table 3 [5].

Table 3. Thermal crack index ( $I_{ct}$ )

Criteria	Crack index
No cracking	$I_{ct} \geq 1.5$
To minimize cracking	$1.2 \leq I_{ct} \leq 1.5$
To minimize harmful cracking	$0.7 \leq I_{ct} \leq 1.2$

### 2.4. Analysis models Results

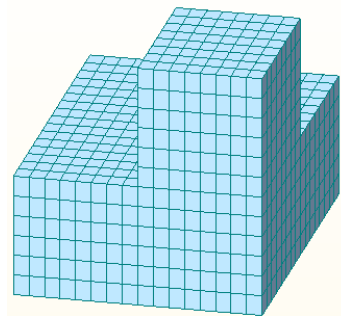


Figure 2. Model geometry of 1/4 concrete piers.

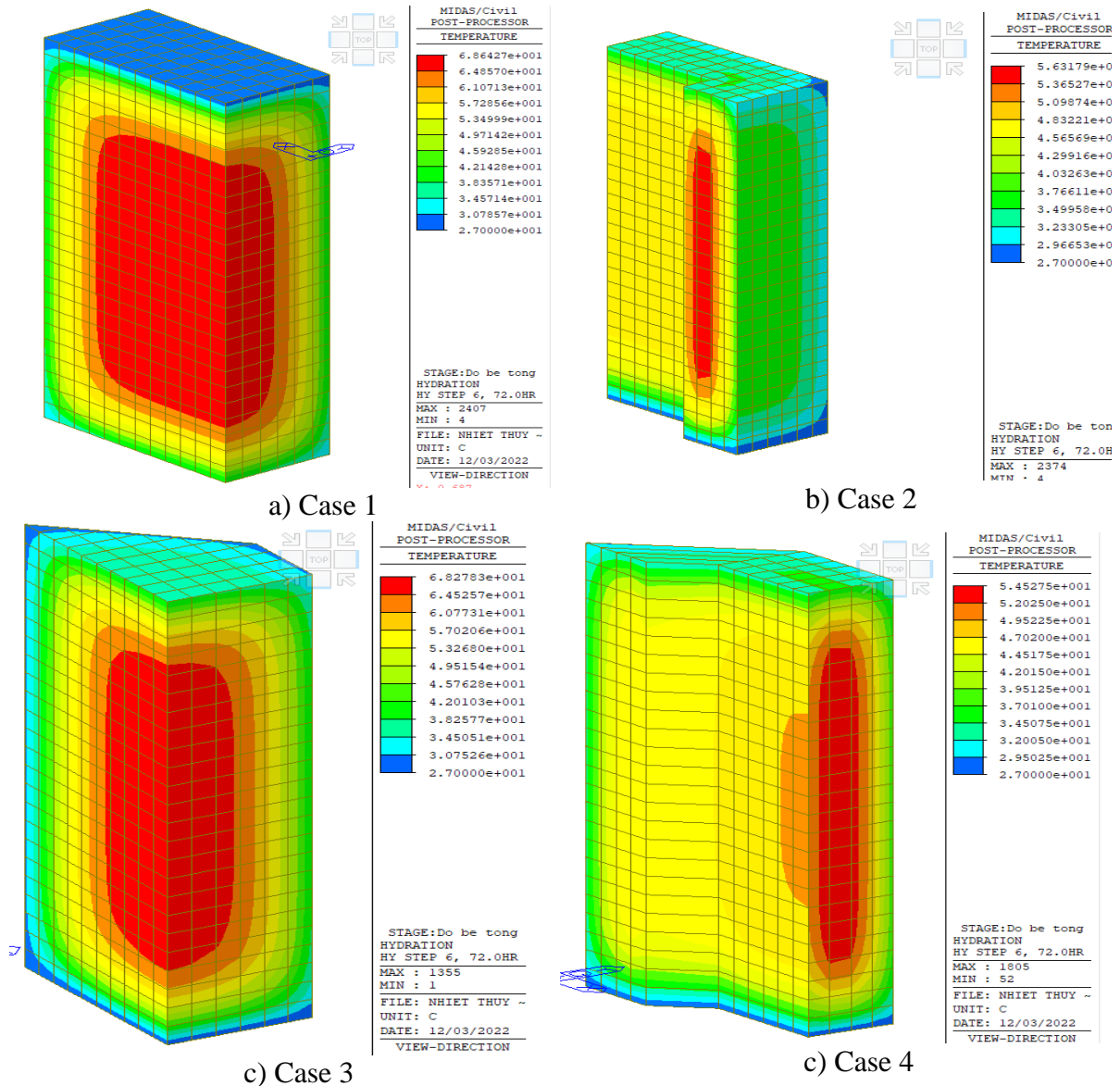


Figure 3. Maximum temperature at the piers center in different piers cross-section shapes 10m×4m×6m at 70 h.

The 3-D FE model was created using the Midas/Civil software. The element used in the thermal analysis is a 3-D eight-node thermal solid element and 3-D six-node thermal solid element, which has one degree of freedom - temperature - at each node. The concrete and foundation in the stress analysis are modeled with a 3-D eight-node structural solid element, which is coupled with the 3-D thermal solid element. The temperature distribution obtained from the thermal analysis is then served as “thermal loading” in the stress calculation. The FE model geometry is depicted in Figure 2.

Figure 3 shows the maximum temperature development at the core of the concrete pier for 4 case of pier cross-section shapes. The maximum temperature, maximum temperature value and temperature difference and its crack index are listed in Table 3. The maximum temperatures at the concrete core are 70.3°C, 56.31°C, 69.51°C and 54.66°C in Cases 1, 2, 3 and 4, respectively. It may be noted that in Case 4, the maximum temperature and temperature difference are the smallest compared to Cases 1,2 and 3. After reaching the peak temperature, it begins to cool

down. Figure 3 and Table 3 together show that the probabilities of cracking in the pier concrete are 51%, 68%, 58% and 103%, in cases 1, 2, 3 and 4, respectively

Table 3. The maximum temperature, temperature difference and its crack index in different pier cross-section shapes.

Case	Max. temperature (°C)	Temperature difference (°C)	Crack index ( $I_{cr}$ )	Occurrence time (h)
1	70.3	43.3	0.51	72
2	56.31	27.95	0.68	48
3	69.51	42.51	0.58	72
4	54.66	27.66	1.03	72

### 3. Artificial Neural Network (ANN) applied to forecast thermal cracking in concrete Pier

#### 3.1 ANN Model

An artificial neural network (ANN) is a one of machine learning model, built to simulate the biological principles of the human brain, consisting of a large number of artificial neurons linked together into a network for information processing. ANN is a simulation technique that is very effective in finding solutions to complex problems that cannot be solved by traditional mathematical models. Therefore, in recent decades, the use of artificial neural networks has been widely applied in many fields [10, 13]

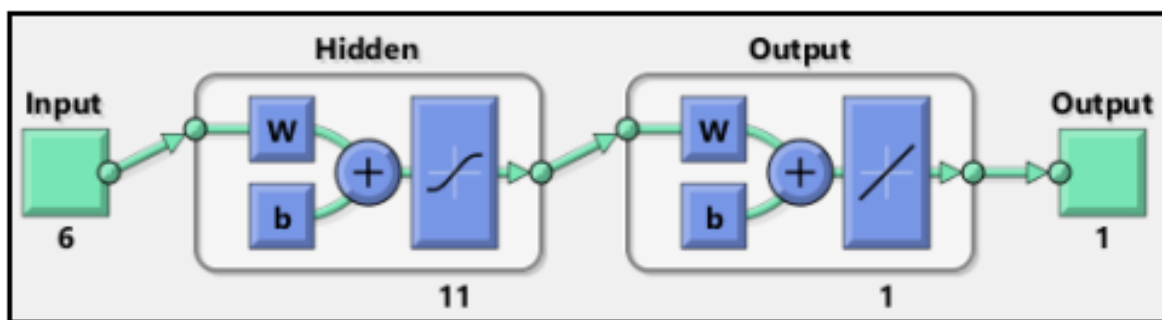


Figure 4. Schematic of artificial neural network model in Matlab [21]

The general structure of an ANN usually includes 3 components: Input layer, Hidden layer and Output layer (Figure 4). Where the input layer is the first layer, the output layer is the last layer and the connection between these two layers is the hidden layer as illustrated in Figure 1. Working like a human brain, ANN are learned by experience and the training phase, have the ability to store, and use them to predict unknown data. During the algorithm training phase, the ANN learns to recognize patterns from the input data, and then compares the generated results

with the desired results. The classic Levenberg - Marquardt algorithm is used to train the network [21]. The number of hidden neurons is selected as the input parameter of the sample. All networks are trained with datasets to select the network with the lowest error. If the lowest error is still high, the number of hidden neurons is increased by 1. Training process using MATLAB software with Neural Network Toolbox [21].

### 3.2 Input and output parameters of ANN model

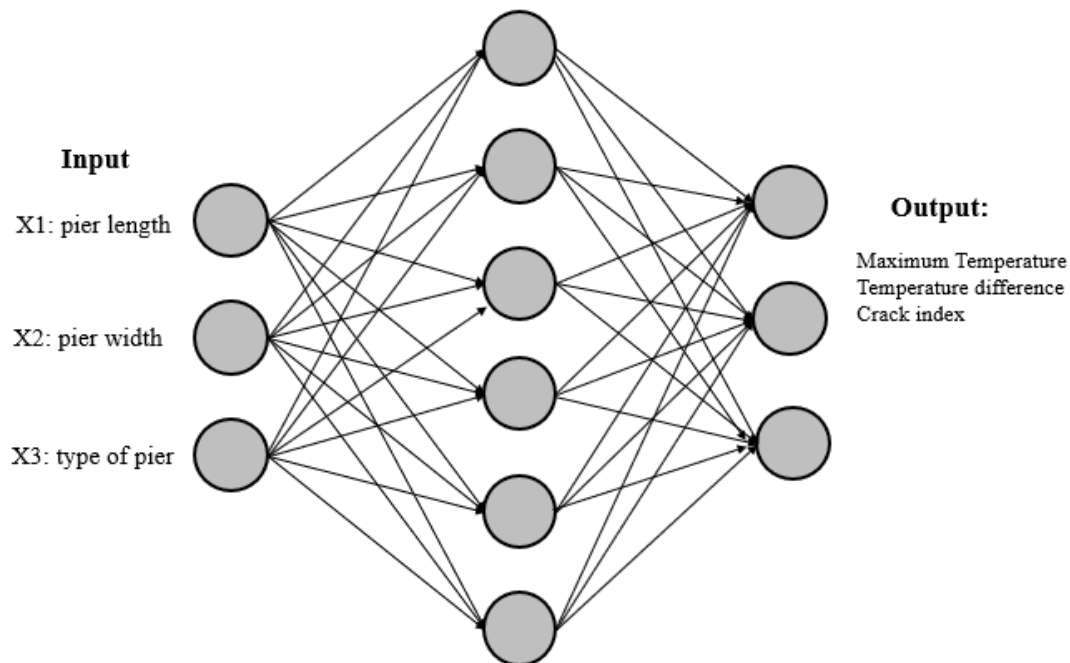


Figure 5. ANN to predict thermal cracking of concrete pier.

As the results in Table 3 and Figure 5 show, parameters such as core temperature, ... depend on the piers cross-section shapes. This article proposes to use the classical Levenberg-Marquardt method to train the network of ANN. With 3 parameters, each parameter is created an ANN network. The ANN network is trained with the following parameters: the number of networks is 3, 3 inputs (X1 - width of pier, X2 - length of pier, X3 - type of pier), 3 output (Maximum temperature, Temperature difference and crack index), one hidden layer. **The type of pier parameter was numbered as 1, 2, 3 and 4 respectively in database.** Number of data samples: total studied data is  $8 \times 4 \times 4 = 128$  samples, 128 training samples and 25 test samples.

### 3.3 Results and discussions

The performance of neural network training was shown in Figure 6. The regression was used, is the classical Levenberg-Marquardt method. The results shown a high regression from 0,99 to 1.



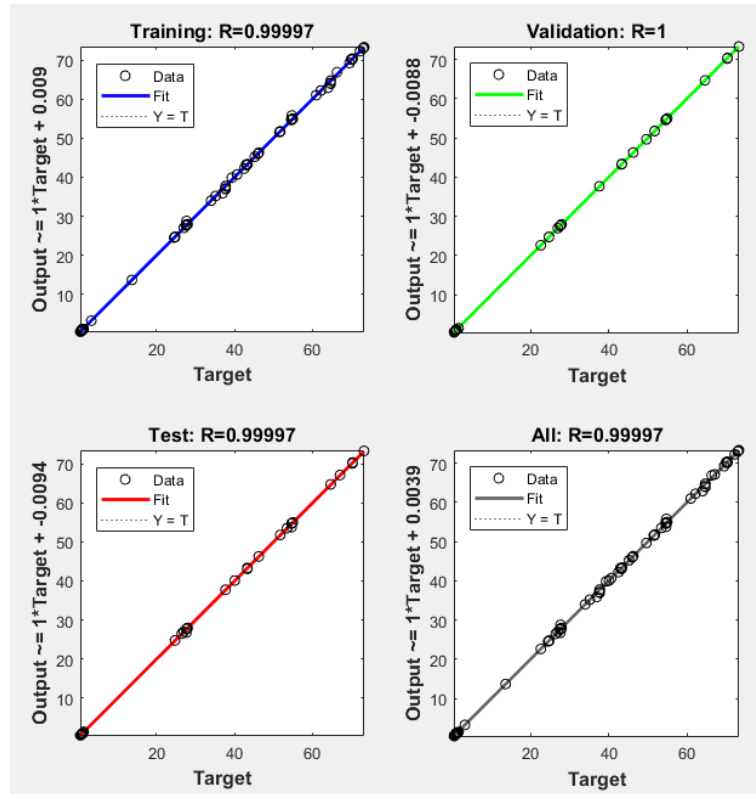


Figure 6. Results of regression after training in ANN.

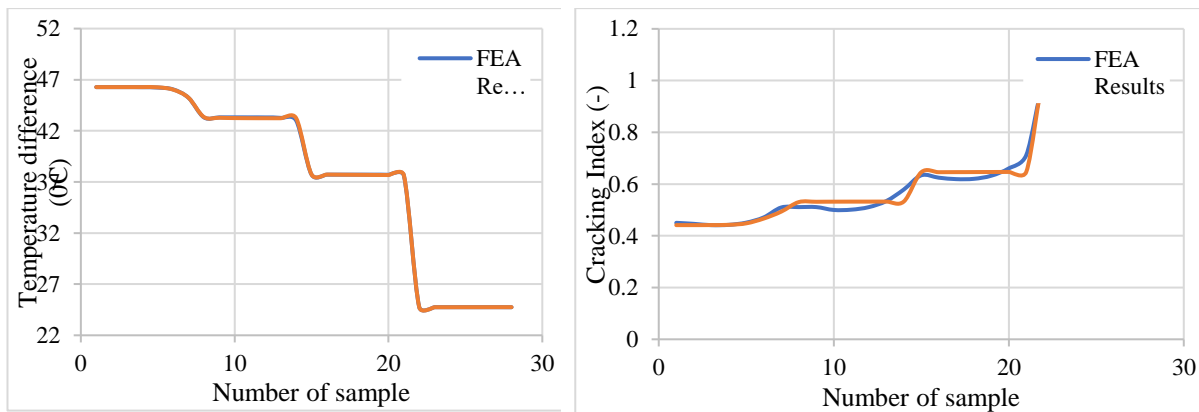


Figure 7. Predict temperature difference and cracking index of concrete pier.

In Figure 7, the ANN network model was built, trained and run, giving predictive results of 3 important parameters (max temperature, temperature difference, cracking index) of the pier concrete from the input data of FEA with high precision. The forecast results are applied to design and choose the appropriate size in minimizing cracks on the pier concrete.

#### 4. CONCLUSIONS

In this study, the ANN network was trained by the classic Levenberg - Marquardt algorithm, can be predicted 3 early-age thermal parameters that influences on thermal cracking in pier masse concrete such as: maximum temperature, temperature difference, cracking index

with high accuracy, the correlation coefficient from 0,99 to 1. The ANN networks can be used to predict the crack on early age of massive concrete pier and help to designer to choose the appropriate size in minimizing cracks on the pier concrete.

Further work should investigate the effect of the initial temperature of concrete, ambient temperature, the construction stage, ... on the crack on early age of massive concrete pier. Some measurement experiments need to be performed to validate the data results in FEA software.

## ACKNOWLEDGMENTS

This research is funded by the University of Transport and Communications (UTC) under grant number T2021-CT-006TD.

## REFERENCES

- [1]. ACI, 116R-90, Cement and Concrete Terminology, Technical Documents, 2000.
- [2]. ACI, 207.1 R-05 Guide to Mass Concrete, 2005.
- [3]. T.A. Do et al., Effects of Thermal Conductivity of Soil on Temperature Development and Cracking in Mass Concrete Footings, *Journal of Testing and Evaluation*, 43 (2015) 20140026. <https://doi.org/10.1520/JTE20140026>
- [4]. T.A. Do et al., Evaluation of heat of hydration, temperature evolution and thermal cracking risk in high-strength concrete at early ages, *Case Studies in Thermal Engineering*, 21 (2020) 100658. <https://doi.org/10.1016/j.csite.2020.100658>
- [5]. T.A. Do, Influence of Footing Dimensions on Early-Age Temperature Development and Cracking in Concrete Footings, *Journal of Bridge Engineering*, 20 (2015) 06014007. [https://doi.org/10.1061/\(ASCE\)BE.1943-5592.0000690](https://doi.org/10.1061/(ASCE)BE.1943-5592.0000690)
- [6]. Institute, J.C., Guidelines for control of cracking of mass concrete, 2016.
- [7]. I. Maruyama, P. Lura, Properties of early-age concrete relevant to cracking in massive concrete, *Cement and Concrete Research*, 123 (2019) 105770. <https://doi.org/10.1016/j.cemconres.2019.05.015>
- [8]. A. Smolana et al., Early age cracking risk in a massive concrete foundation slab: Comparison of analytical and numerical prediction models with on-site measurements, *Construction and Building Materials*, 301 (2021) 124135. <https://doi.org/10.1016/j.conbuildmat.2021.124135>
- [9]. V.T. Luu et al, Research on thermal cracking control in mass concrete by using cooling pile system, *Journal of Science and Technology in Civil Engineering*, 13 (2019) 99-107. [https://doi.org/10.31814/stce.nuce2019-13\(3V\)-11](https://doi.org/10.31814/stce.nuce2019-13(3V)-11)(in Vietnamese)
- [10].M. Rasul, A. Hosoda, Prediction of occurrence of thermal cracking of RC abutments using artificial neural networks., 65A (2019) 560-568. <https://doi.org/10.11532/structcivil.65A.560>
- [11].Y. Sargam et al., Predicting thermal performance of a mass concrete foundation – A field monitoring case study, *Case Studies in Construction Materials*, 11 (2019) e00289. <https://doi.org/10.1016/j.cscm.2019.e00289>
- [12].Y. Sargam et al, Machine learning based prediction model for thermal conductivity of concrete, *Journal of Building Engineering*, 34 (2021) 101956. <https://doi.org/10.1016/j.jobbe.2020.101956>
- [13].S. Bhokha, S.O. Ogunlana, Application of artificial neural network to forecast construction duration of buildings at the predesign stage, *Engineering, Construction and Architectural Management*, 6 (1999) 133-144. <https://doi.org/10.1108/eb021106>
- [14].H. B. Ly et al., Compressive strength prediction of recycled aggregate concrete by artificial neural network, *Transport and Communications Science Journal*, 72 (2021) 369-383. <https://doi.org/10.47869/tcsj.72.3.11>(in Vietnamese)

- [15].T.A Do et al, Forecasting thermal cracking risk in early-age concrete bridge piers using artificial neural net-works, Journal of Science and Technology in Civil engineering, 16 (2022) 139-150. [https://doi.org/10.31814/stce.huce\(nuce\)2022-16\(5V\)-12](https://doi.org/10.31814/stce.huce(nuce)2022-16(5V)-12) (in Vietnamese)
- [16].A. Ghajar, Y. Cengel, Heat and Mass Transfer - Fundamentals and Applications, 6th Edition, McGraw-Hill Education, New York, NY, 2020, 2021.
- [17].Z. Zhao, et al., Creep and thermal cracking of ultra-high volume fly ash mass concrete at early age, Cement and Concrete Composites, 99 (2019) 191-202. <https://doi.org/10.1016/j.cemconcomp.2019.02.018>
- [18].MIDAS, Heat of Hydration – Analysis Manual. MIDAS Information Technology, 2011.
- [19].N.K. Ho, C.C. Vu, Analysis of temperature field and thermal stress in mass concrete using FEA method, Journal of Science and Technology in Civil engineering, 6 (2012) 17-27. (in Vietnamese)
- [20].ACI, 318-19, Building Code Requirements for Structural Concrete (ACI 318-14) and Commentary, 2014.
- [21].Mathworks, Global Optimization Toolbox: User's Guide (r2015b), 2015.